Lasers in Surgery and Medicine 24:346–359 (1999)

Detection of Transplant Vasculopathy in a Rat Aortic Allograft Model by Fluorescence Spectroscopic Optical Analysis

Alexander Christov, PhD,[1] Erbin Dai, MD,[1] Liying Liu, MD,[1] Leslie W. Miller, MD,[2] Piers Nash, BSc,[3] Alshad Lalani, BSc,[3] Grant McFadden, PhD,[1,3] Patric N. Nation, DVM,[4] John Tulip, PhD,[5] and Alexandra Lucas, MD[1,3]*

[1]Vascular Biology Group, John P. Robarts Research Institute, University of Western Ontario, London, Ontario N6A 5B8, Canada
[2]Division of Cardiology, University of Minnesota, Minneapolis, Minnesota 55455-0213
[3]Department of Microbiology and Immunology, University of Western Ontario, London, Ontario N6A 5B8, Canada
[4]Department of Lab Animal Services, University of Alberta, Edmonton, Alberta T6G 2M7, Canada
[5]Department of Electrical Engineering, University of Alberta, Edmonton, Alberta T6G 2M7, Canada

Background and Objective: **Transplant vasculopathy is a leading cause of late cardiac graft loss. We have examined laser-induced fluorescence (LIF) spectroscopy as an optical diagnostic tool for detection of intimal plaque development and inflammatory cellular invasion in a rat model of aortic allograft transplant.**
Study Design/Materials and Methods: **Infrarenal aortic segments were transplanted from Lewis to Sprague Dawley rats. A range of vasculopathy development was produced by treatment with a viral anti-inflammatory protein. LIF spectra were recorded from the intima of aortic implants at 28 days. Fluorescence intensity was analyzed for correlation with vasculopathy development.**
Results: **Significant differences in LIF intensity at 400–450 nm ($P \leq 0.05$ by ANOVA) were detected. LIF emission was correlated with plaque growth ($R^2 = 0.980$), vessel narrowing ($R^2 = 0.964$), and cellular invasion ($R^2 = 0.971$) by regression analysis.**
Conclusion: **LIF optical analysis provides a nontraumatic diagnostic approach for detection of atherosclerosis prior to cardiac transplant or during development of vasculopathy after transplant. Lasers Surg. Med. 24:346–359, 1999.**

Key words: atherosclerosis; inflammation; laser; rejection; transplant

INTRODUCTION

Transplant vasculopathy is a diffuse atheromatous process that occludes coronary arteries, producing ongoing ischemic damage to the heart [1,2]. This is the leading cause of cardiac graft loss after the first year post transplant [3,4]. Ischemic injury occurring at the time of transplantation [2,5] and chronic ongoing inflammatory and im-

Contract grant sponsor: Photonics Research Ontario; Contract grant sponsor: the Heart and Stroke Foundation of Canada; Contract grant sponsor: the J. P. Robarts Research Institute.

*Correspondence to: Alexandra Lucas, MD, Robart's Research Institute, University of Western Ontario, 100 Perth Drive, PO Box 5015, London, Ontario N6A 5K8, Canada. E-mail: arl@rri.on.ca

Accepted 15 February 1999

mune reactions [6–8] after cardiac transplant are believed to produce continuing injury to the arterial wall. Growth of coronary atheromatous lesions, present in donor heart vessels prior to transplant, may also contribute to the development of occlusive arterial disease post transplant [8].

Transplant ishemia is often silent, due to the loss of sensory innervation after cardiac transplantation. The lack of anginal symptoms makes detection of transplant vasculopathy difficult. Vasculopathy is often detected only after significant cardiac injury has already occurred, or is discovered incidentally at follow-up angiography or by intravascular ultrasound. However, both contrast angiography and intravascular ultrasound have limited sensitivity for the detection of transplant atherosclerosis or associated cellular inflammatory changes. Contrast angiography detects changes in the arterial lumen diameter at sites of stenosis but can miss generalized vascular narrowing [8,9]. Intravascular ultrasound (IVUS) can identify plaque growth and gross morphological changes, but does not detect cellular invasion, or specific changes in lipid or thrombus in the arterial wall [10,11]. Similarly, magnetic resonance imaging (MRI) remains significantly limited by motion artifacts produced by the beating heart [12–14]. The capacity of other optical imaging systems, such as Raman spectroscopy [15,16] and Optical coherence tomography (OCT) [17] for detection of transplant vasculopathy or rejection have not, to date, been assessed.

Current medical management for transplant atherosclerosis is limited to control of hyperlipidemia [18,19] and acute rejection [3,7,20] and remains only partially effective. Surgical interventions such as coronary artery bypass surgery [21,22] and angioplasty [23] are also limited by the diffuse nature of transplant vasculopathy and the often delayed diagnosis, necessitating repeat transplant in many cases [24]. New approaches to treatment with medications such as rapamycin [25,26] and angiopeptin [27] are promising therapeutic approaches but remain under investigation.

Recent reports have suggested that laser angioplasty and/or irradiation are effective in treating long diffuse chronic atherosclerotic vascular lesions [28] and potentially reducing smooth muscle cellular proliferation [29]. The laser light used for angioplasty simultaneously induces light emission from naturally fluorescing compounds on the arterial surface. When laser light is applied at a lower energy level, fluorescence emission can be used as a diagnostic instrument for detection of developing atherosclerosis. In the clinical setting laser-induced fluorescence (LIF) of native fluorophors has been developed and used successfully to locate tumors [30–32], dental caries [33], ophthalmologic disorders [34], dermal lesions [35], cardiac nodal tissue [36], and atherosclerotic plaque [37–43]. Very recently LIF spectroscopic detection of transplant rejection in endomyocardial biopsy specimens from cardiac transplants in a rat model has been reported [44]. LIF has also been developed for guidance during laser angioplasty [38,45].

Spectroscopic examination of the arterial intima has been demonstrated to detect changes in plaque composition [43,46], specifically collagen [43], elastin [46], and lipid content [40] as well as thrombosis [47]. Remodeling of the arterial wall with atherosclerotic plaque growth requires new synthesis, as well as breakdown, of fibrous tissues. Macrophage invasion is facilitated by release of proteolytic enzymes that degrade collagen and elastin in fibrous tissues. Collagen and elastin are dominant natural fluorophors in arterial tissue. Thus plaque growth and inflammatory cell responses are expected to alter collagen and elastin content and hence fluorescence emission in the arterial wall.

Early identification of transplant vasculopathy or extensive vascular mononuclear cell invasion prior to cardiac damage, as well as assessment of therapeutic approaches or guidance during angioplasty, would be potentially helpful in preventing or treating transplant associated vasculopathy. Detection of atherosclerotic lesions in donor hearts prior to transplant would also be of benefit in allowing early aggressive, preventative therapy or potentially assisting in the choice of donor organs for implant. The use of a nontraumatic fluorescence optical analysis system may provide a new approach for early detection and treatment of transplant vasculopathy.

We have examined LIF spectroscopy as a potential optical diagnostic tool for the detection of transplant vasculopathy and inflammatory cell invasion into the arterial wall following transplantation in a rat aortic allograft model.

MATERIALS AND METHODS

Rat Model of Aortic Allograft Transplant

The rat model of aortic allograft transplant vasculopathy has been reported elsewhere (Miller

L. et al., unpublished observation). However, in order to explain the studies performed, a brief description of this technique is given [48]. Thirty Sprague Dawley rats had infrarenal transplant of aortic segments taken from 15 Lewis rats (SD/L). All groups of rats were anesthetized for surgery using general pentobarbital anesthetic (6.5 mg per 100 g weight, Somnotrol, MTC Pharmaceuticals, Cambridge, Ontario, Canada) given by intraperitoneal (i.p.) injection. A 2.0 cm section of Lewis rat aorta was resected from below the renal arteries to the iliac bifurcation. The Sprague Dawley rat aorta was isolated by clips placed proximal and distal to the planned implant site, below the renal arteries. The aorta between the two vessel clips was cut out and a 1.0 cm aortic section from a Lewis rat was transplanted into each of two Sprague Dawley rat aortas using end to end implantation (e.g., one Lewis rat aorta was divided and used for transplant into two Sprague Dawley rats).

Protein or saline was infused into the tail vein once blood flow to the aorta returned, as assessed by visible pulsation of the transplanted aortic segment after removal of the surgical clips. The viral anti-inflammatory protein SERP-1 [49] and control saline infusions were given in a total volume of 1.0 ml, as a one-time dose, immediately after transplant; saline control (seven rats) and SERP-1 at doses of 0.3 ng/rat (six rats), 3.0 ng/rat (six rats), 30 ng/rat (five rats), and 300 ng/rat (six rats). Seven rats (five Sprague Dawley and two Lewis rats) had Sprague Dawley to Sprague Dawley (SD/SD) or Lewis to Lewis (L/L) control isograft transplants under the same general anesthetic conditions with 1.0 ml saline infusion into the tail vein.

At four weeks follow-up, animals were euthanized with 1.0 ml euthanyl per kg (114 mg of pentobarbitol per kg; MTC Pharmaceuticals, Canada Packers Inc., Cambridge, Ontario, Canada). All research protocols and general animal care conform to the Guiding Principles for Animal Experimentation as determined by the Canadian Council on Animal Care.

Laser-Induced Fluorescence Spectroscopy

Native tissue fluorescence emission was induced by monochromatic laser light using an AIS Dymer 200+ XeCl excimer (308 nm) laser (Advanced Interventional Systems, Irvin, CA) operating at 1.4 mJ/pulse, 5 Hertz. The excimer laser light was coupled to a 7F (French) laser angioplasty ring catheter (CeramOptec, Bonn, Germany). For spectroscopy, the catheter was held perpendicular and aposed to the tissue surface (spot size 2,500 μm^2) with angle and position controlled by a three-dimension-motion-freedom micrometer stage (J.A. Noll Co., Monroeville, PA). Fluorescence emission spectra were recorded with an EG & G Princeton Applied Research Model 1462 Optical Multichannel Analysis system (Toronto, Ontario, Canada) equipped with a Model 1228-HR-320 Instruments SA, Inc. spectrograph (Edison, NJ) and a Model 1455-700 HQ intensified photodiode array (EG & G Princeton Applied Research). The Optical Multichannel Analysis system was coupled to a Power MacIntosh 9500/200 computer with Kestrel OMA (Rhea Corporation, Wilmington, DE) software for data acquisition and analysis. A Schott WG-360 sharp cutoff filter was positioned between the detection fiber and the spectrograph input slit in order to reduce interference from scattered ultraviolet excitation light (Fig. 1A). The system was calibrated with a model 6047 mercury vapor lamp (Oriel Corporation, Stratford, CT) prior to performing each experiment. Background signal (constant for each recording series) was subtracted from each spectrum for optical and electronic noise correction. A photodiode trigger High Speed Silicon Detector DET 200, ThorLabs, Inc. (Newton, NJ) has been added to synchronize fluorescence recording to the onset of the laser pulse, limiting fluorescence recording to the time during which fluorescence emission was detected after the laser excitation pulse. Excitation energy was measured at the output end of the excitation fiber with a Coherent Labmaster E power meter (Auburn, CA).

Spectra were recorded from 37 aortic specimens post transplant. Specimens were frozen at –80°C and thawed at room temperature immediately prior to recording LIF spectra. Saline was dropped onto the arterial sections to prevent excessive drying during the recording of fluorescence spectra. Twenty fluorescence emission spectra (every spectrum a sum of 10 individual ones in series) were recorded from the intimal surface of each aortic transplant specimen.

Viral Anti-Inflammatory Protein Purification and Source

SERP-1 was produced from a recombinant Chinese hamster ovary (CHO) cell line (a kind gift from Dr. L. Ling, Biogen, Inc.) by affinity chromatography [50]. Affinity resin was produced by linking monoclonal antibody (mAb) AXB7.9 (courtesy of Biogen, Inc.) to CNBr-activated Sepharose-4B (Pharmacia) according to the manufacturers' instructions, at a ratio of 5 mg of protein

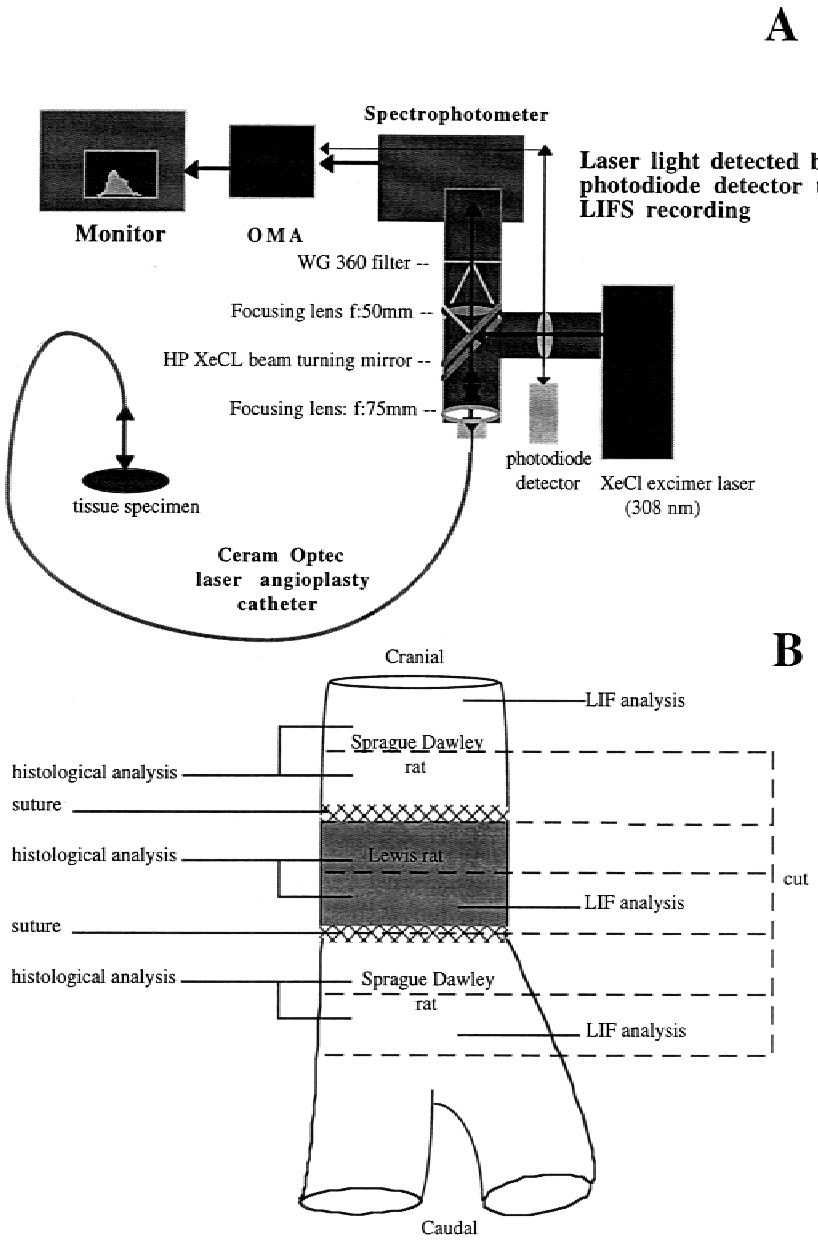

Fig. 1. Experimental set-ups. **A:** Diagram depicting the laser-induced fluorescence spectroscopy single fiber system used for these experiments. Laser light at 308 nm is deflected by a beam turning mirror (HP XeCL beam turning mirror) and focused onto a 7F laser angioplasty ring catheter for excitation of tissue fluorescence. Emitted fluorescence is gathered into the same fiber and focused onto the Model 1228-HR-320 Instruments SA, Inc. spectrograph through a Shott WG 360 filter. Fluorescence recording is triggered by the photodiode High Speed Silicon Detector DET 200 detector placed at the emission port of the laser to provide simultaneous onset of laser pulses and spectroscopic recording by the EG & G Princeton Applied Research Model 1462 Optical Multichannel Analysis system. **B:** Diagram indicating processing of aortic allograft specimens harvested from the SD/L transplant rats for histological and LIF analyses.

per ml of resin. Supernatant from SERP-1 expressing CHO cells (pH 7.5–8.0) was mixed with AXB7.9-Sepharose resin for two hours at room temperature. The resin was then loaded onto a column and washed with 15 column volumes of phosphate buffered saline (PBS), followed by 15 column volumes of PBS + 1 M NaCl, and a final wash step of 15 column volumes of PBS. SERP-1 was eluted from the column with 25 mM H_3PO_4, pH 2.8 into a tube containing 25 μl of 3M Tris-HCl, pH 7.9 per ml of eluent. The resulting highly purified SERP-1 was greater than 95% pure as judged by overloaded Coomassie stained SDS-PAGE gels and the appearance of a single peak on reverse-phase HPLC. The concentration of purified SERP-1 was determined by absorbance at 280 nm using a molar extinction coefficient of 32,700 M−1cm−1 as described [50].

Histology and Morphometric Analysis

Aortic specimens 3.0 cm in length were removed, encompassing both the transplant surgery site (1.0 cm aorta from the donor) and 1.0 cm above and below the suture lines. The harvested transplant segments were then divided into three sections of equal lengths (1.0 cm) taken from the proximal, mid, and distal parts of the trans-

planted aorta (Fig. 1B). The top and bottom sections were taken such that these sections spanned 50% or more of the suture lines, e.g., the sites of anastomosis of the transplanted (Lewis aorta) section. The middle sections originated from the transplanted Lewis aortic segment. The sections were divided into two. Half of each specimen was used for spectroscopic interrogation and the adjacent half was directly fixed in neutral buffered formalin for histological analysis. LIF spectra were recorded from the proximal and distal halves of the top and bottom sections respectively, and subsequently fixed with hematoxylin and eosin for microscopic and morphometric examination. All specimens were then fixed in 10% sodium phosphate buffered formalin, processed, impregnated, and embedded in paraffin and cut into 5 μm sections by microtome as previously described [49,51]. A total of six cross-sections per rat taken from the aortic transplant site were cut and stained for each specimen.

The section with the largest detectable area of atherosclerotic plaque was outlined using a Sony Power HAD 3CCD color video camera attached to a Zeiss Axioskop using the Empix Northern Eclipse trace application program (Empix Imaging Inc., Mississauga, Ontario, Canada). Each system was calibrated to the microscopic objective used. All histologic sections were independently assessed by a veterinary pathologist (PNN), who was blinded to the treatment given to each transplanted rat.

Statistics

The originally recorded spectra, after an equalizing baseline correction, were normalized by dividing fluorescence intensity at all wavelengths by the maximum intensity, providing intensity values ranging from 0–1.0. This approach is necessary due to inequalities in the amplitude of the originally recorded spectra, produced by minor variations in optical alignment and instrumental interference, which are not related to specific tissue fluorescence. The variability proved to be statistically insignificant with respect to differences detected in the fluorescence emission recorded from specific experimental groups (data not shown). Mean fluorescence emission intensity at the wavelengths examined was derived for each rat and values were used for all statistical analyses. Changes in normalized LIF at wavelengths selected in the known specific optical fluorescence emission range (for excitation with 308 nm) of atherosclerotic plaque were examined and assessed for significance by analysis of variance (ANOVA). Difference spectra comparing, $dI/d\lambda$ values vs. wavelength plotting and polynomial regression analysis were used to evaluate changes in spectral shape. No statistically significant difference was observed when comparing LIF emission, as well as structural characteristics of the rat aorta, from the donor and recipient segments in the SD/L allograft transplant controls (data not shown, $P > 0.432$).

Mean values representing each rat were used for analysis of aortic structural characteristics. The mean values for plaque area and area of mononuclear cell invasion in the intimal and adventitial layers of the aortic transplant sections were analyzed by Student's unpaired t-test or by analysis of variance (ANOVA).

LIF and aortic structural characteristics were compared using simple and multiple regression analysis as has been previously described [43]. Measured plaque area, and areas of inflammatory cell invasion in the arterial wall, as well as the calculated vessel narrowing—[Total IEL (internal elastic lamina) area – intimal area] × 100/Total IEL area—were compared with normalized fluorescence emission intensity at selected wavelengths, representing the areas of the spectra with the greatest visible changes associated with infusion of the anti-inflammatory protein SERP-1, at 10 nm increments between 400 nm and 490 nm.

Statview (Berkley, CA), a MacIntosh statistics package, was used for calculation of means, standard error, and significance by ANOVA, t-test, and regression analysis.

RESULTS

Altered LIF With Viral Anti-Inflammatory Therapy

The intensity of natural fluorescence emission induced by 308 nm laser light excitation of the intimal surface of rat aortic specimens is a composite of overlapping specific fluorescence bands, emitted by individual tissue constituents. The fluorescence spectra recorded are characterized by an increase at 370 nm, a maximum at 380–390 nm, and a smooth decline ($y = a - bx + cx^2$; $R^2 > 0.99$) in intensity between 390 nm and 440 nm (Fig. 2).

Treatment with SERP-1 (3–300 ng/rat), a viral anti-inflammatory serine proteinase inhibitor that has been demonstrated to reduce atherosclerotic plaque and early macrophage invasion [49],

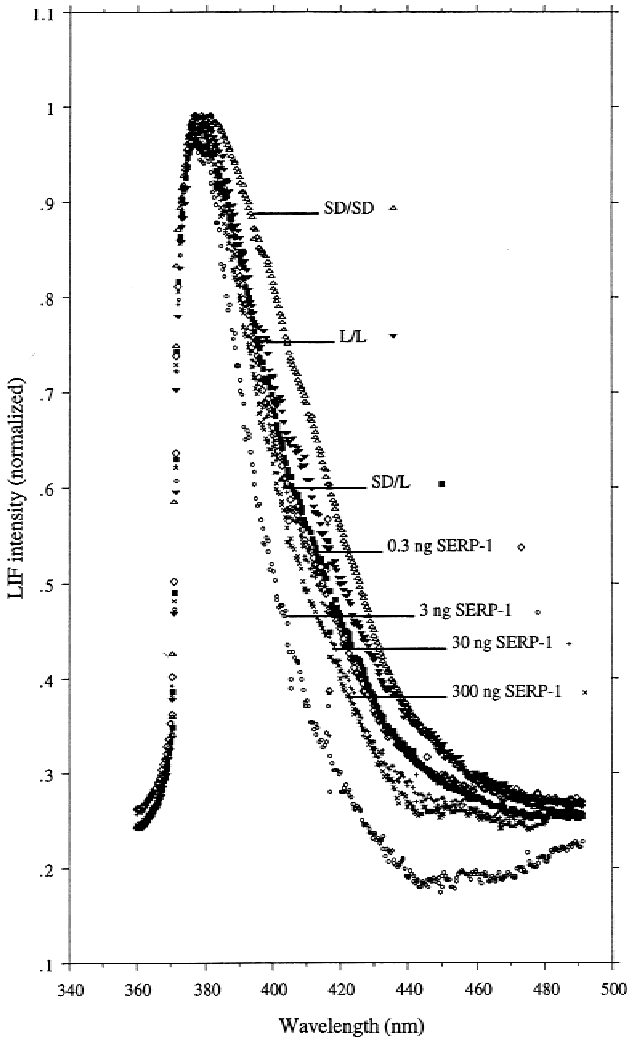

Fig. 2. Mean fluorescence emission spectra recorded from rat aortic transplant sections 4 weeks after surgery at 308 nm excimer laser excitation. The LIF intensity on the Y axis is normalized by dividing intensity at each wavelength by the maximal intensity recorded in individual spectra. A reduction in the fluorescence emission intensity at 400–440 nm is detected after treatment with increasing doses of viral anti-inflammatory protein (SERP-1) infusion.

produced a decrease in LIF intensity recorded from transplanted aortic specimens at 400–450 nm on comparison with saline control infusion in SD/L allograft transplants, SD/SD, and L/L isograft control transplants. Specific effects on LIF spectra were seen with increasing concentrations (0.3–300 ng/rat) of SERP-1.

Infusion of SERP-1 changed the spectral emission shape at this wavelength range, as demonstrated by difference spectra comparison and by plotting calculated dI/dλ values vs. wavelength (Fig. 3). Difference spectra (data not shown) were calculated by subtraction of normalized mean LIF intensity spectra recorded from the SERP-1 treated samples and from the mean spectra recorded from the SD/L, SD/SD, and L/L controls. Statistical analysis showed significant differences between dI/dλ values representing different treatments and control specimens at the selected wavelengths (intervals of 10 nm) assessed, with the greatest reduction in dI/dλ produced by a concentration of 3 ng SERP-1 per rat ($P \leq 0.05$).

Treatment with 3 ng SERP-1 significantly lowers LIF emission intensity values at the same selected wavelengths in comparison with the SD/L control (at 400 nm and 420 nm) and the SD/SD isograft transplants control (at 400 nm, 410 nm, 420 nm, 430 nm, and 440 nm) as assessed by ANOVA (Table 1). A significant decrease in LIF intensity was also seen with 300 ng SERP-1 treatment at 400 nm and 410 nm compared to SD/SD controls. Treatment with the rest of the SERP-1 concentrations showed a very small effect compared to the controls.

Correlation of Specific LIF Emission Intensity Profiles With Structural Characteristics of Transplant Vasculopathy

The effects of treatment with the anti-inflammatory protein SERP-1 on plaque growth, vessel narrowing (stenosis), and invasion of mononuclear cells, as measured by morphometric analysis of the rat aortic transplant specimens (Fig. 4), were compared to the corresponding changes in fluorescence emission. The parameters of plaque development (plaque cross-section area and related arterial stenosis) were found to be significantly larger in the SD/L controls when compared to SERP-1 treatment at all concentrations, as well as to the SD/SD and L/L isograft controls (Fig. 5A,B). There were significant areas of mononuclear cellular invasion detectable in the intimal and adventitial layers post allograft (SD/L) transplant. These areas were markedly reduced after SERP-1 infusion (Fig. 5C,D). Mononuclear cell invasion was also significantly lower in the isograft controls (except for the adventitial layer of the SD/SD control).

Simple regression analysis was applied to parallel mean values of the structural characteristics of all treatment variants to the corresponding fluorescence emission intensity values at the wavelengths selected at 10 nm intervals in the 400–490 nm range (Table 2). However, the SD/L saline treated control aortic specimens, characterized with the greatest plaque growth and cell in-

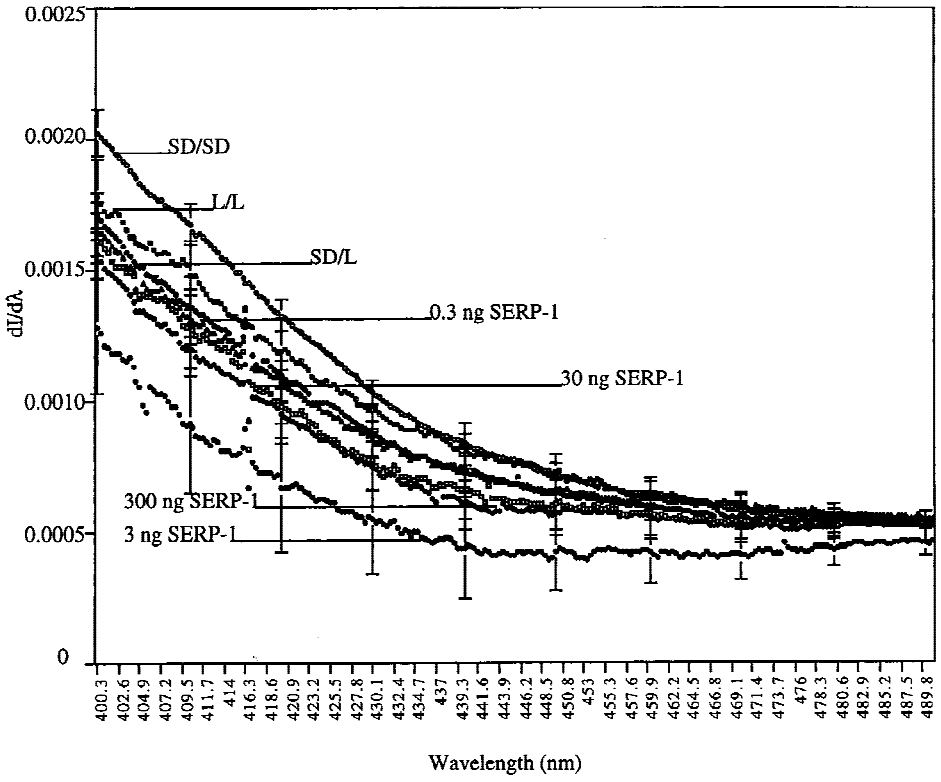

- L/L $Y = .046 - 1.893E^{-4} * X + 1.982E^{-7} * X^2$; $R^2 = .995$
- SD/L $Y = .047 - 1.980E^{-4} * X + 2.091E^{-7} * X^2$; $R^2 = .992$
- SD/SD $Y = .058 - 2.424E^{-4} * X + 2.546E^{-7} * X^2$ $R^2 = .996$
- 0.3 ng SERP-1 $Y = .045 - 1.897E^{-4} * X + 2.011E^{-7} * X^2$; $R^2 = .984$
- 3 ng SERP-1 $Y = .050 - 2.108E^{-4} * X + 2.251E^{-7} * X^2$; $R^2 = .975$
- 30 ng SERP-1 $Y = .047 - 2.005E^{-4} * X + 2.143E^{-7} * X^2$; $R^2 = .981$
- 300 ng SERP-1 $Y = .045 - 1.912E^{-4} * X + 2.071E^{-7} * X^2$; $R^2 = .968$

Fig. 3. Changes in the curve shape of recorded LIF emission spectra, produced by treatment with the anti-inflammatory and anti-atherosclerotic agent SERP-1, demonstrated by plotting dI/dλ values against the corresponding wavelengths and polynomial regression analysis (equations).

vasion, did not exhibit the highest fluorescence emission, as expected.

Thus, a correlation between the plaque-development parameters and the LIF intensity values was found after the SD/L controls group was excluded from the analysis (Table 2, Fig. 6). Further analysis is therefore necessary to accurately assess inflammatory cellular responses in the transplant segments.

Regression Analysis of LIF Emission Intensity at Multiple Wavelengths

As far as the LIF intensity values are assumed to be an integral quantitative measure, representing all naturally fluorescing compounds in the arterial surface, multiple regression analysis of the relationship between LIF intensity values and structural characteristics of the inflammatory process and plaque deposition, is a promising analytical approach. Multiple regression analysis also allows the development of formulae that may be used to detect and differentiate areas of intimal plaque development and mononuclear cell invasion associated with transplant vasculopathy. The use of LIF values from wavelength ranges that correlate with collagen and elastin fluorescence emission has already been proven successful for the detection of correlations between natural fluorophor concentrations and changes in LIF emission spectra.

Analyzing the relationship between LIF intensity values from all recorded LIF spectra at

TABLE 1. Mean Values of 308 nm Excited LIF Emission Intensity From Rat Aortic Intimal Surface

	Control SD/L		SERP-1 0.3 ng		SERP-1 3 ng		SERP-1 30 ng		SERP-1 300 ng		SD/SD		L/L	
Wavelength	LIF	Std. Err.	LIF	Std. Err.	LIF	Std. Err.	LIF	Std. Err.	LIF	Std. Err.	LIF	Std. Err.	LIF	Std. Err.
400 nm	.682[a]	.035	.655	.032	.512[ab]	.101	.645	.058	.626[c]	.039	.808[bc]	.035	.714	.055
410 nm	.558	.048	.538	.038	.376[b]	.110	.524	.063	.490[c]	.043	.687[bc]	.031	.607	.054
420 nm	.460[a]	.042	.453	.032	.282[ab]	.104	.412	.061	.400	.040	.556[b]	.026	.498	.056
430 nm	.375	.037	.366	.029	.236[b]	.089	.332	.050	.322	.041	.444[b]	.019	.421	.036
440 nm	.324	.039	.319	.027	.192[b]	.085	.287	.047	.264	.042	.368[b]	.015	.363	.038
450 nm	.292	.033	.298	.025	.191[b]	.070	.273	.044	.256	.039	.327[b]	.015	.327	.031
460 nm	.274	.026	.291	.028	.193	.056	.262	.037	.255	.036	.293	.012	.295	.027
470 nm	.262	.021	.278	.024	.193	.046	.254	.033	.243	.029	.273	.010	.277	.026
480 nm	.250	.020	.270	.020	.207	.032	.253	.027	.247	.018	.259	.008	.269	.012
490 nm	.253	.013	.270	.014	.223	.025	.255	.027	.255	.013	.256	.007	.264	.008

[abc]Differences between values marked with identical indexes e.g., a,b,c, are statistically significant ($P < 0.05$) at given wavelength.

three selected ranges of the spectra (400–429 nm, 430–460 nm, and 461–490 nm—1 nm intervals between the individual readings) and structural characteristics of transplant vasculopathy per rat, a statistically significant correlation for LIF emission intensity with plaque cross-section area for the range 430–460 nm ($R^2 = 0.980$) was found (Table 3). LIF emission intensity also tends to correlate with the plaque cross-section area (in the range of 461–490 nm), as well as with the vessel stenosis (in the ranges of 430–460 nm and 461–490 nm), but the obtained lower adjusted R^2 values suggest lower correlations due to variation in the measured numbers.

The extent of cellular invasion exhibits a positive correlation ($R^2 = 0.886$ for the intimal layer and $R^2 = 0.945$ for the adventitial layer in the range of 461–490 nm) with the LIF emission. However, the current lack of knowledge about the specific optical properties of the invading cells prevents the assessment of additional considerations of their contribution to the entire process of autofluorescence at this point.

DISCUSSION

We have examined the capacity of laser-induced fluorescence spectroscopy of natural fluorophores for detection of transplant vasculopathy in a rat model of aortic allograft transplant, and more specifically transplant associated mononuclear cell invasion. Local arterial wall inflammation with cellular invasion and plaque formation have the potential to change the proportions of autofluorescent compounds on the aortic inner surface. Arteries undergoing atherosclerotic growth exhibit an altered autofluorescence profile that may reflect the fluorescent properties of the lipoproteins [40] or connective tissue [43,46] accumulating in the tissue. Collagen and elastin are considered the major natural arterial fluorophores detected after ultraviolet excitation and their local content correlates with histological and biochemical properties of normal aortic intima, atherosclerotic plaque growth, and inflammatory cellular invasion [40,42,43]. Fluorescence emission intensity profiles of normal aortic wall and transplant induced atheromatous plaques excited by excimer laser excitation at 308 nm were found to differ significantly.

Treatment with 3 ng/rat SERP-1 was found to significantly reduce LIF intensity compared to the SD/L allografts and SD/SD isograft controls at certain wavelengths, visibly changing the shape of the autofluorescence emission spectra. It also caused the greatest reduction in plaque area and mononuclear cell invasion in the adventitial layer (Fig. 5), despite the fact that differences established between structural characteristics among the SERP-1 treated variants themselves, were not proven statistically significant. After treatment with 300 ng/rat, lower LIF intensity values were observed compared to the SD/SD controls at 400 nm and 410 nm. The concentration of 30 ng/rat appears to be less effective in this respect, although all four doses of SERP-1 reduced plaque area and inflammatory cell invasion. Judging by the structural characteristics after SERP-1 treatment, concentrations of 30 ng/rat and 300 ng/rat were associated with plaque development at magnitudes of approximately the same value as the lowest concentration (0.3 ng/rat) used, which had

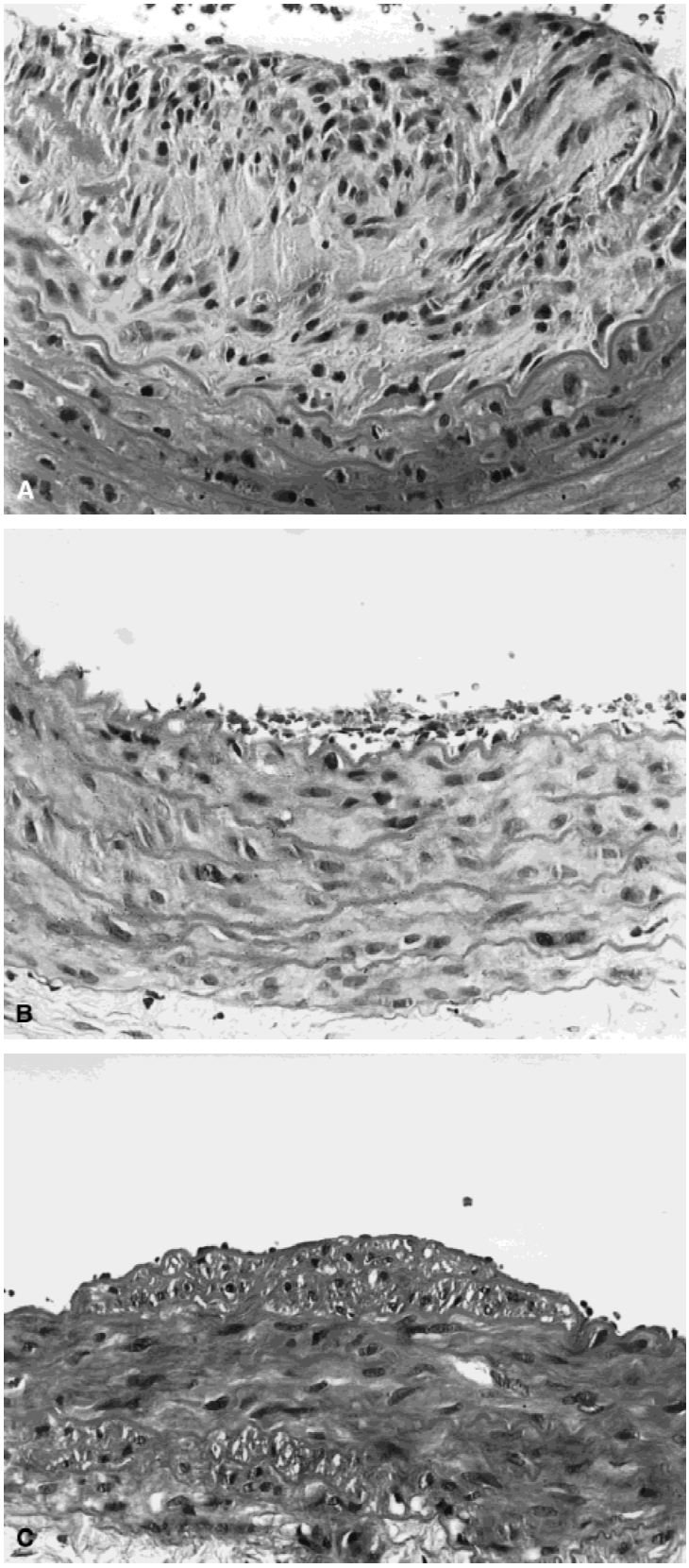

Fig. 4. Hematoxylin and eosin stained histology sections taken from rat aorta after transplant taken at 4 weeks follow-up (Magnification 400×). **A:** Saline control treated section of aorta demonstrating marked intimal hyperplasia and mononuclear cell invasion into the intimal and the medial layers of the aorta wall. **B:** Aortic section post transplant after infusion of SERP-1 (3 ng/rat) with reduced intimal proliferation and reduced cellular invasion into the intimal and medial layers. **C:** Isograft control (SD/SD) aortic section with reduced intimal hyperplasia and cell invasion.

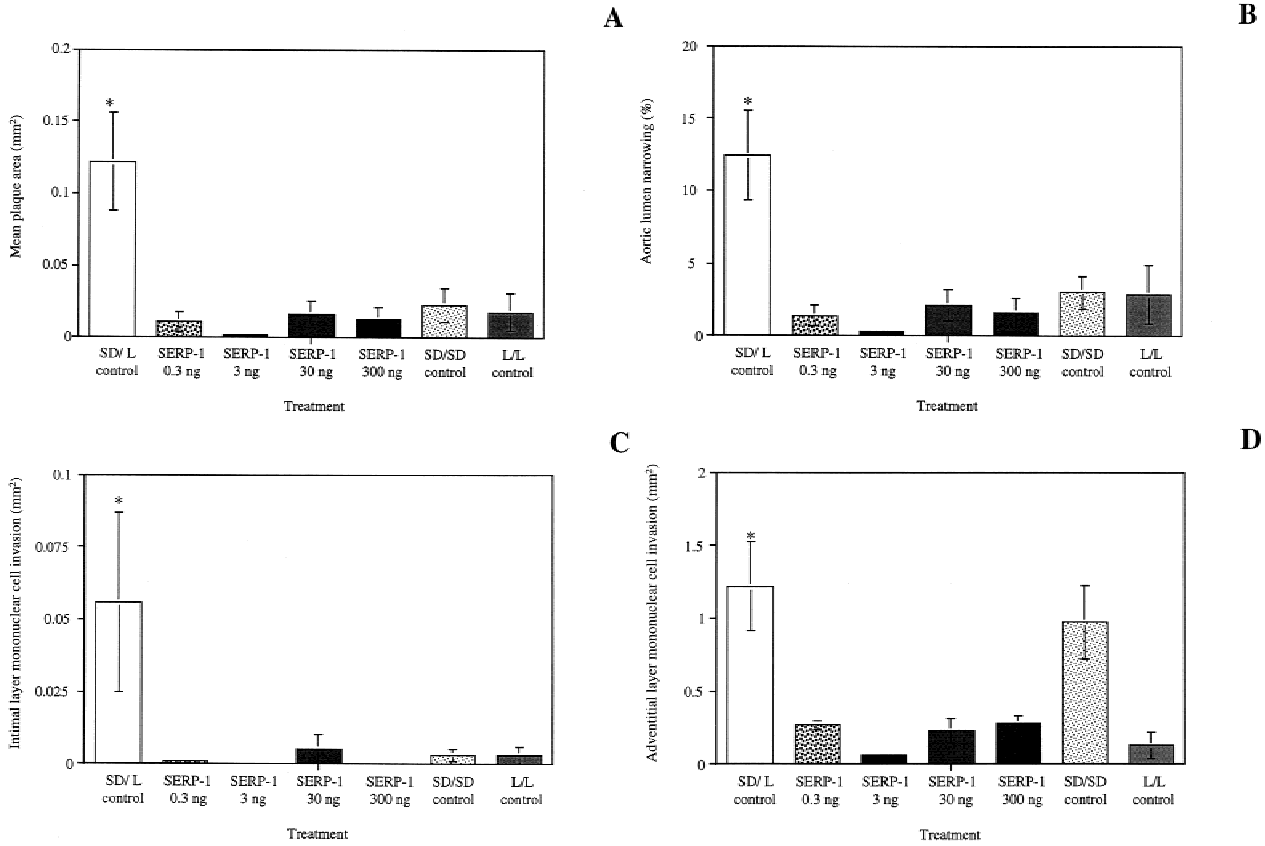

Fig. 5. Bar graph demonstrating significant reductions in mean plaque area (**A**), arterial stenosis (**B**), intimal (**C**), and adventitial (**D**) layer mononuclear cell invasion with SERP-1 infusion (*P <0.05 when compared to the SD/L control) as determined by morphometric analysis.

TABLE 2. Correlation Coefficients (R^2) Obtained in Simple Regression Analysis Comparing LIF Intensity Values to Transplant Vasculopathy Structural Characteristics

	LIF 400 nm	LIF 410 nm	LIF 420 nm	LIF 430 nm	LIF 440 nm	LIF 450 nm	LIF 460 nm	LIF 470 nm	LIF 480 nm	LIF 490 nm
Plaque area: all variants	.055	.053	.068	.067	.087	.062	.056	.063	.014	.010
Plaque area: all variants excluding control SD/L	.884	.892	.851	.838	.836	.854	.815	.793	.719	.600
Vessel narrowing (stenosis): all variants	.085	.084	.103	.105	.130	.100	.082	.097	.032	.023
Vessel narrowing (stenosis): all variants excluding control SD/L	.867	.902	.894	.899	.918	.927	.852	.829	.762	.615

no effect on the LIF intensity. Whereas the result of treatment with 0.3 ng/rat could be due to insufficiency of the anti-inflammatory agent delivered to the organism, the effects of the higher doses of SERP-1 detected by histological and fluorescence analyses might be a result of increased inflammation due to immune reactions against foreign proteins.

Variable degrees of vasculopathy were induced by treating rats, at the time of transplant, with a viral anti-inflammatory protein known to inhibit atheroma formation and inflammatory cell invasion in this model (L. Miller et al., 1998, submitted for review). LIF spectroscopy reproducibly detected atheroma development ($P \leq 0.05$) [49] in this rat aortic transplant model. Atherosclerotic plaque growth is consistent with an altered LIF emission spectral curve shape [38]. In our experiments, changes in the fluorescence emission spectral shape between 400 nm and 490 nm produced

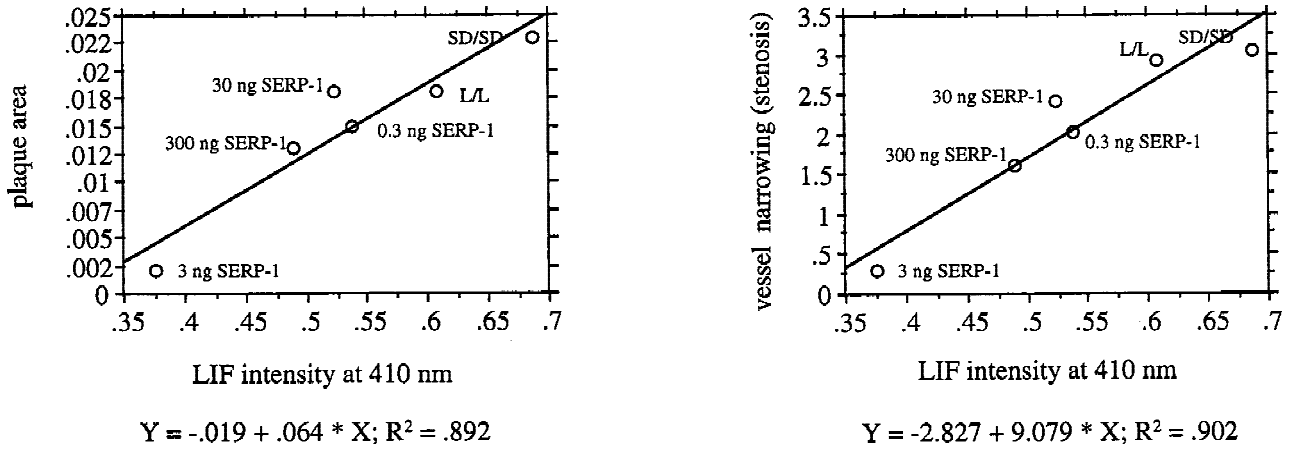

Fig. 6. Simple regression analysis plots exhibiting the correlation between the mean values of LIF emission intensity at 410 nm with the mean values of measured plaque area and artery narrowing.

TABLE 3. Correlation Coefficients (R^2) Obtained in Multiple Regression Analysis Comparing LIF Intensity Values to Transplant Vasculopathy Structural Characteristics (All Variants)

	LIF at selected wavelengths (1 nm interval) from:					
	400 nm to 429 nm		430 nm to 460 nm		461 nm to 490 nm	
	R^2	Adjusted R^2	R^2	Adjusted R^2	R^2	Adjusted R^2
Plaque area	.807	—	.980	.853	.960	.597
Vessel narrowing (stenosis)	.771	—	.964	.732	.936	.364
Mononuclear cell invasion—intimal layer	.807	—	.772	—	.886	.785
Mononuclear cell invasion—adventitial layer	.899	—	.971	.780	.945	.454

by treatment with SERP-1, as assessed by comparison of the difference spectra, by dI/dλ values vs. wavelength and by polynomial regression analysis, were the first indication that LIF emission intensity variations were related to altered vasculopathy development. The differences in fluorescence emission intensity at the selected wavelengths detected and the correlation established with mean specific values of plaque formation related parameters, as well as the results of the multiple regression analysis, reached another level of accuracy for monitoring transplant vasculopathy changes by LIF examination. The SD/SD and L/L isografts had reduced plaque and inflammatory cell invasion (Fig. 5) and increased LIF emission intensity compared to the SD/L controls. This fact focused our attention on the intensive inflammatory cell invasion in the intimal surface layer of the SD/L controls. The mean area occupied in cross-section by the mononuclear cells in the intimal layer is in the range of up to 43% of the plaque area. The rat aortic wall in the abdominal aorta is a thin, nearly translucent structure that facilitates detection of autofluorescence from all layers. Mononuclear cells in the intimal layer might be predicted to act as a screen, or inner filter, absorbing and/or scattering some portion of the transmitted fluorescence emission, as well as excitation light—and hence reducing the net LIF emission intensity. This could be a possible explanation for the fact that a correlation by simple regression analysis between the mean values of LIF and the plaque development structural characteristics was observed only when the SD/L controls group was not considered in the analysis. Despite the statistically insignificant correlation between characteristics of the structure and LIF intensity in some of the spectral regions analyzed (Table 3), our results strongly suggest that the level of inflammatory cellular invasion directly, or indirectly, affects autofluorescence emission (with an 89% predictive value, $R^2 = 0.886$) when the entire LIF spectrum is analyzed by multiple regression analysis. It should also be noticed that in the rat aorta, which is a very small and thin walled structure, adventitial cellular invasion may be expected to produce a direct change in LIF emission, whereas in human coronary transplant

arteriopathy increased mononuclear cell invasion might contribute by an overall alteration in arterial structure and composition with generally increased inflammation.

Laser-induced fluorescence spectroscopy may therefor provide a sensitive and specific approach to the early detection of coronary atheroma for the detection of plaque prior to transplant, as well as for the detection of accelerated transplant vasculopathy and vascular inflammation after cardiac transplant. Detection of inflammatory cell infiltrates in the coronary arterial wall may also correlate with chronic transplant rejection providing a nontraumatic optical biopsy for therapeutic guidance. There are at present limited diagnostic systems, specifically contrast angiography, intravascular ultrasound (IVUS), and magnetic resonance imaging (MRI) for detection of transplant vasculopathy. IVUS and Optical coherence tomography (OCT) have not been demonstrated to detect specific chemical changes in plaque growth, although they do detect some precise but limited structural changes associated with plaque growth. Neither IVUS, OCT, nor MRI has been reported to detect inflammatory cell invasion in the artery wall.

Further studies will be necessary to assess the capacity of this LIF spectroscopy system for early detection of transplant atherosclerosis in a blood field. However, the use of a single fiber system with apposition of the fiber to the arterial face may minimize blood effects on LIF emission [52]. Detection of a correlation between mononuclear cell invasion and chronic transplant rejection post cardiac transplant will require comparative studies with endomyocardial biopsy or coronary atherectomy specimens for actual application as a diagnostic technique. This optical biopsy approach, however, has the potential to reduce the need for endomyocardial excisional biopsy, in addition to angiography and IVUS, at long term follow-up.

Spectral pathology, including various spectroscopic techniques such as reflectance, fluorescence, infrared absorption, and Raman spectroscopy are recognized as having advantages on comparison with histopathological analysis of diseased tissue [53] such that information can be gathered in situ; light signals from all parts of the body can be delivered by a remote access and data can be collected and analyzed in a fraction of a second, allowing possible real time feed back. Some disadvantages of surgical biopsy that include unnecessary removal of tissue from larger areas, a lack of representative sampling of suspected diseased tissues, greater expenses and consumption of time, can be avoided by using optical biopsy methods. In addition, spectroscopic signals may detect biochemical changes, that often precede the morphological changes observed in histology [53].

Laser-induced fluorescence optical analysis may provide a nontraumatic approach for the early detection of transplant vasculopathy, for guidance of laser treatment of transplant occlusions, and for evaluation of new therapeutic approaches to transplant atherosclerosis.

ACKNOWLEDGMENTS

We thank The London Health Sciences Center for providing the AIS Dymer 200+ laser and Ceram Optec for providing the 7F laser angioplasty ring catheters. We also thank Drs. Maria Drangova and David Holdsworth for valuable discussions, Dr. Leona Ling and Biogen, Inc. for supplying the viral serpin, as well as Ms. Carol Walton for helping with the typing of this manuscript.

REFERENCES

1. Miller L, Kobashigawa J, Valantine H, Ventura H, Hauptman P, O'Donnell J, Wiedermann J, Yeung A. The impact of cyclosporine dose and level on the development and progression of allograft coronary disease. Sandoz/CVIS Investigators. J Heart Lung Transplant 1995;14:227–234.
2. Constanzo MR, Naftel DC, Pritzker MR, Heilman JK, Boehmer JP, Brozena SC, Dec GW, Ventura HO, Kirlin JK, Bourge RC, Miller LW. The Cardiac Transplant Research Database. Heart transplant coronary artery disease detected by coronary angiography: A multi institutional study of preoperative donor and recipient risk factors. J Heart Lung Transplant 1998;17:744–753.
3. Uretsky BF, Griffith BP, Murali S, Hardesty RL, Reddy PS, Trento A, Rabin B, Bahnson HT, Lee A. Development of coronary artery disease in cardiac transplant patients receiving immunosuppressive therapy with cyclosporine and prednisone. Circulation 1987;76:827–834.
4. Hosenpud JD, Bennet LE, Keck BM, Fiol B, Bouchek MM, Novick RJ. The registry of the international society of heart and lung transplantation: Fifteen official report. J Heart Lung Transplant 1998;17:656–668.
5. Tilney NL, Whitley WD, Tullius SG, Heemana UW, Wasowska B, Baldwin WM 3rd, Hancock WW. Serial analysis of cytokines, adhesion molecule expression and humoral responses during development of chronic kidney allograft rejection in a new rat model. Transplant Proc 1993;25:861–862.
6. vonWillebrand E, Jurcic V, Isoniemi H, Hayry P, Paavonen T, Krogerus L. Adhesion molecules and their ligands in chronic rejection of human renal allografts. Transplant Proc 1997;29:1530–1501.

7. Hayry P, Myllarniemi M, Aavik E. Chronic allograft rejection. Transplant Proc 1996;28:2337–2338.
8. Tuzcu EM, De Franco AC, Goormastic M, Hobbs RE, Rincon G, Bott-Silverman C, Mc Carthy P, Stewart R, Mayer E, Nissen SE. Dichotomous pattern of coronary atherosclerosis 1 to 9 years after transplantation: insights from systematic intravascular ultrasound imaging. J Am Coll Cardiol 1996;27:839–846.
9. Tuzcu EM, Hobbs RE, Rincon G. Occult and frequent transmission of atherosclerotic coronary disease with cardiac transplantation: insights from intravascular ultrasound. Circulation 1995;91:1706–1713.
10. Verkin CS, White RA, Donayre CE, Kopcho HGE. The ideal guidance imaging system for endovascular interventions. J Cardiovasc Surg 1996;37 (Suppl 1):5–9.
11. Nissen SE, De Franco AC, Tuzcu EM, Moliterno DJ. Coronary intravascular ultrasound: diagnostic and interventional applications. Cor Artery Dis 1995;6:355–367
12. Vallabhajosula S, Fuster V. Atherosclerosis: imaging techniques and the involving role of nuclear medicine. J Nucl Med 1997;38:1788–1795.
13. Correia LCL, Altar E, Heleman MD, Ocali O, Hutchins GM, Fleg JL, Gerstenblithy G, Zerhouni EA, Li Ma JAC. Intravascular magnetic resonance imaging of aortic atherosclerotic plaque composition. Art Thromb Vasc Biol 1997;17:3626–3632.
14. Trouard TP, Altbach MI, Hunter GC, Esttelson CD, Gmitro AF. MRI and NMR spectroscopy of the lipids of atherosclerotic plaque in rabbits and humans. Magn Reson Med 1997;30:19–26.
15. Brennan III JF, Romer TJ, Lees RS, Tercyak AM, Kramer Jr. JR, Feld MS. Determination of human coronary artery composition by Raman spectroscopy. Circulation 1997;96:99–105.
16. Romer TJ, Brennan III JF, Fitzmaurice M, Feldstein ML, Deinum G, Myles JL, Kramer JR, Lees RS, Feld MS. Histopathology of human coronary atherosclerosis by quantifying its chemical composition with Raman spectroscopy. Circulation 1998;97:878–885.
17. Brezinski ME, Tearney GJ, Bouma BE, Izatt JA, Hee MR, Swanson EA, Southern JF, Fujimoto JG. Optical coherence tomography for optical biopsy: properties and demonstration of vascular pathology. Circulation 1996; 93:1206–1213.
18. Kobashigawa JA, Katznelson S, Laks H, Johnson JA, Yeatman L, Wang XM, Chia D, Terasaki PI, Sabad A, Cogert GA, Trosian K, Hamilton MA, Moriguchi JD, Kawata N, Hage A, Drinkwater DC, Stevenson LW. Effect of pravastatin on outcomes after cardiac transplantation. N Engl. J Med 1995;333:621–627.
19. Lucas A, Dai E, Liu LY, Nation PN. Atherosclerosis in Marek's Disease Virus infected hypercholesterolemic roosters is reduced by HMGCoA Reductase and ACE inhibitor therapy. Card Res 1998;38:237–246.
20. Tilney NL. Thoughts on the immunobiology of chronic allograft rejection. [Review]. Transplant Proc 1995;27: 2123–2125.
21. Halle AA 3rd, DiSciascio G, Massin EK, Wilson RF, Johnson MR, Sullivan HJ, Bourge RC, Kleinman NS, Miller LW, Aversano TR, Wray RB, Hunt SA, Weston MW, Davies RA, Rincon G, Crandall CC, Cowley MJ, Kubo SH, Fisher SG, Vetrovec GW. Coronary angioplasty, atherectomy and bypass surgery in cardiac transplant recipients. J Am Coll Cardiol 1995;26:120–128.
22. Miller LW, Donohue TJ, Wolford TA. The surgical management of allograft coronary disease: a paradigm shift. (Review) Seminars Thorac Cardiovasc Surg 1996;8:133–138.
23. Patel VS, Radovancevic B, Springer W, Frazier OH, Massin E, Benrey J, Kadipasaoglu K, Cooley DA. Revascularization procedures in patients with transplant coronary artery disease. Eur J Cardiothorac Surg 1997;11: 895–901.
24. Fiane AE, Klow NE, Simonsen S, Levorstad K, Geiran O. Percutaneous transluminal angioplasty and retransplantation due to transplant coronary artery disease. Scand Cardiovasc J 1997;31:223–227.
25. Schmid C, Heeman U, Azuma H, Tilney NL. Rapamycin inhibits transplant vasculopathy in long-surviving rat heart allografts. Transplantation 1995;60:729–733.
26. Kobashigawa JA. Targeting nonalloimmune-dependent pathways. (Review) Transplant Proc 1997;29(8A):47S–50S.
27. Wahlers T, Mugge A, Oppelt P, Heublein B, Fieguth HG, Jurmann MJ, Uthoff K, Haveric A, Albes JM, Foegh M, Borst HG. Preventive treatment of coronary vasculopathy in heart transplantation by inhibition of smooth muscle cell proliferation with angiopeptin. J Heart Lung Transplant 1995;14:143–150.
28. Litvack F, Eigler N, Margolis J, Rothbaum D, Bresnahan JF, Holmes D, Untereker W, Leon M, Kent K, Pichard A, King S, Ghazzal Z, Cummins F, Krauthamer D, Palacios I, Block P, Hartzler GO, O'Neill W, Cowley M, Roubin G, Klein LW, Framkel PS, Adams C, Goldenberg T, Laudenslager J, Grundfest WS, Forrester JS for the ELCA investigators. Percutaneous excimer laser coronary angioplasty: Results in the first consecutive 3,000 patients. J Am Coll Cardiol 1994;23:323–329.
29. Sumpio BE, Li G, Deckelbaum LI, Gasparro FP. Inhibition of smooth muscle cell proliferation by visible light-activated psoralen. Circ Res 1994;75:208–213.
30. Lam S. Bronchoscopic, photodynamic, and laser diagnosis and therapy of lung neoplasms. Curr Opin Pulm Med 1996;2:271–276.
31. Schomacker KT, Frisoli JK, Richter JM, Deutsch TF, Nishioka NS. Discrimination of adenomatous from hyperplastic colonic polyps *in-vitro* by laser-induced fluorescence. Lasers Surg Med 1990;(Suppl) 2:5.
32. Ramanujam N, Mitchel MF, Mahadevan A, Warren S, Thomsen S, Silva E, Richards-Kortum R. In vivo diagnosis of cervical intraepithelial neoplasia using 337 nm excited laser-induced fluorescence. Proc Natl Acad Sci USA 1994;91:10193–10197.
33. Colvard MD, Pick RM. Future directions of lasers in dental medicine. Curr Opin Periodontol 1993;144–150
34. Phillips AF, McDonnell PJ. Laser-induced fluorescence during photoreactive keratectomy: a method for controlling epithelial removal. Am J Ophthalmol 1997;123: 42–47.
35. Leffell DJ, Stetz ML, Milstone LM, Deckelbaum LI. In vivo fluorescence of human skin. A potential marker of photoaging. Arch Dermatol 1988;124:1514–8.
36. Perk M, Flynn GJ, Gulamhusein S, Wen Y, Smith C, Bathagate B, Tulip J, Parfrey NA, Lucas A. Laser-induced fluorescence identification of sinoatrial and atrioventricular nodal conduction tissue. PACE 1993;16: 1701–1712.
37. Deckelbaum LI, Lam JK, Cabin SH, Clubb KS, Long MB.

Discrimination of normal and atherosclerotic aorta by laser induced fluorescence. Lasers Surg Med 1987;7:330–335.
38. Leon MB, Lu DY, Prevosti LG, Macy WW, Smith PD, Granovsky M, Bonner FR, Balban RS. Human arterial surface fluorescence: Atherosclerotic plaque identification and effect of laser atheroma ablation. J Am Coll Cardiol 1988;12:94–102.
39. Garrand TJ, Stetz ML, O'Brien KM, Gindi GR, Laifer LI, Deckelbaum LI. Characterization of the site dependency of normal canine arterial fluorescence. Lasers Surg Med 1990;10:375–383.
40. Oraevski AA, Jacques SL, Pettit GH, Sauerbrey RA, Tittel FK, Nguy JH, Henry PD. XeCl laser-induced fluorescence of atherosclerotic arteries: spectral similarities between lipid-rich lesions and peroxidized lipoproteins. Circ Res 1993;72:84–90.
41. Baraga JJ, Rava PR, Taroni P, Kittrell C, Fitzmaurice M, Feld MS. Laser induced fluorescence spectroscopy of normal and atherosclerotic human aorta using 306–310 nm excitation. Lasers Surg Med 1990;10:245–261.
42. Baraga JJ, Rava RP, Fitzmaurice M, Tong LL, Taroni P, Kittrell C, Feld MS. Characterization of the fluorescent morphological structures in human arterial wall using ultraviolet-excited microspectrofluorimetry. Atherosclerosis 1991;88:1–14.
43. Yan W, Perk M, Chagpar A, Wen Y, Stratoff S, Schneider WJ, Jugdutt BI, Tulip J, Lucas A. Laser-induced fluorescence: III. Quantitative analysis of atherosclerotic plaque content. Lasers Surg Med 1995;16:164–168.
44. MacAulay C, Whitehead P, McManus B, Zeng H, Wilson-McManus J, MacKinnon N, Morgan DC, Dong C, Gerla P, Kenyon J. Organ transplant tissue rejection: detection and staging by fluorescence spectroscopy. Presented at BiOS'98, Int'l. Symp. On Biomedical optics, San Jose, California, January 24–30, 1998.
45. Deckelbaum LI, Desai SP, Kim C, Scott JJ. Evaluation of fluorescence feedback system for guidance of laser angioplasty. Lasers Surg Med 1995;16:226–234.
46. Laifer LI, O'Brien KM, Stetz ML, Gindi GR, Garrand TJ, Deckelbaum LI. Biochemical basis for the difference between normal and atherosclerotic arterial fluorescence. Circulation 1989;80:1893–1901.
47. Deckelbaum LI. Laser-assisted angioplasty of inferior vena caval obstructions: what's good for the artery is good for the vein. Hepatology 1989;9:338–9.
48. Mennander A, Raisanen A, Poavonene T, Hayry P. Chronic rejection in the rat aortic allograft. V. Mechanism of the angiopeptin (CBIM 23014C) effect on the generation of allograft atherosclerosis. Transplantation 1993;55:124–128.
49. Lucas L, Liu L, Macen J, Nash P, Dai E, Stewart M, Graham K, Etches W, Boshkov L, Nation PN, Humen D, Lundstrom Hobman M, McFadden G. Virus-encoded serine proteinase inhibitor SERP-1 inhibits atherosclerotic plaque development after balloon angioplasty. Circulation 1996;94:2890–2900.
50. Nash P, Whitty A, Handwerker J, Macen J, McFadden G. Inhibitory specificity of the anti-inflammatory myxoma virus serpin, SERP-1. J Biol Chem 1998;273:20982–20991.
51. Dai E, Steward M, Ritchie B, Mesaeli N, Raha S, Kolodziejczyk D, Lundstrom Hobman L, Liu LY, Etches W, Nation N, Michalak M, Lucas A. Calreticulin, a potential vascular regulatory protein, reduces intimal hyperplasia after arterial injury. Atheroscl Thromb Vasc Biol 1997; 17:2359–2368.
52. Lucas AR, Gauthier T, Clark RH, Isner JM. Angiograpic contrast media interference with laser-induced fluorescence excitation and detection in atheroslerotic human coronary arteries. Am Heart J 1991;121:110–118.
53. Zonios G, Cothren R, Crawford JM, Fitzmaurice M, Manoharan R, Van Dam J, Feld MS. Spectral pathology. Ann N Y Acad Sci 1998;838:108–115.